DEUTSCHES ELEKTRONEN-SYNCHROTRON DESY

DESY SR-75/15
October 1975

Photoabsorption Coefficient of Alloys of Al with Transition Metals V, Fe, Ni and with Cu and Pr from 30 eV to 150 eV Photon Energy

by

H.-J. Hagemann
II. Institut für Experimentalphysik der Universität Hamburg

W. Gudat and C. Kunz
Deutsches Elektronen-Synchrotron DESY, Hamburg

2 HAMBURG 52 · NOTKESTIEG 1

To be sure that your preprints are promptly included in the
HIGH ENERGY PHYSICS INDEX ,
send them to the following address (if possible by air mail) :

DESY
Bibliothek
2 Hamburg 52
Notkestieg 1
Germany

subject classification: 20.1; 21.1; 21.1.1

Photoabsorption Coefficient of Alloys of Al with Transition Metals V, Fe, Ni and with Cu and Pr from 30 eV to 150 eV Photon Energy

H.-J. Hagemann[+]

II. Institut für Experimentalphysik der Universität Hamburg,

2 Hamburg 50, Germany

and

W. Gudat[++] and C. Kunz

Deutsches Elektronen-Synchrotron DESY, 2 Hamburg 52, Germany

The absorption coefficient of VAl_3, FeAl, NiAl, $NiAl_3$, $CuAl_2$, $PrAl_2$ and of disordered V-Al (16 at. % Al, 28 %, 41 %) and Fe-Al (11 %) alloys has been measured in the region of the $M_{2,3}$-absorption of the transition metals and the L-absorption of Al. The strong changes of the Al spectrum in the region of the 100 eV maximum upon alloying are explained as another evidence of the EXAFS (extended x-ray absorption fine structure) nature of these structures. The broad, prominent absorption peaks from the 3p excitations in V and Fe and from the 4d excitations in Pr are influenced only little on alloying and thus appear to be of atomic origin. The fine structure at the onset of the Pr 4d-transitions is identical in the metal and the alloy but differs from that of Pr oxide. The only $M_{2,3}$-edge which is detectably shifted is that of Ni (up to 2.1 eV), whereas the onset of the Al $L_{2,3}$-edge is shifted in all the alloys (up to 1.1 eV). The shifts are interpreted in accordance with x-ray fluorescence and nuclear resonance measurements as changes of the density of states in the valence band of the alloys.

Submitted to Physica Status Solidi

Der Absorptionskoeffizient von VAl_3, FeAl, NiAl, $NiAl_3$, $CuAl_2$, $PrAl_2$ und ungeordneter V-Al (16 at. % Al, 28 %, 41 %) und Fe-Al (11 %) Legierungen wurde im Bereich der $M_{2,3}$-Absorption der Übergangsmetalle und der L-Absorption des Al gemessen. Die starke Veränderung des Al-Spektrums im Bereich des 100 eV-Maximums bei allen Legierungen kann als unterschiedliche Streuung der auslaufenden Elektronenwelle (EXAFS) verstanden werden. Die breiten, prominenten Absorptionsmaxima der 3p Anregungen in V, Fe und der 4d Anregungen in Pr werden durch das Legieren wenig beeinflußt und scheinen daher atomaren Ursprungs zu sein. Die Feinstruktur am Einsatz der Pr 4d-Übergänge ist im Metall und in der Legierung identisch, unterscheidet sich aber von der in Pr Oxyd. Von den $M_{2,3}$-Kanten ist nur der Einsatz der Ni-Kante deutlich verschoben (bis zu 2,1 eV), während der Einsatz der Al $L_{2,3}$-Kante in allen Legierungen verschoben ist (bis zu 1,1 eV). Diese Verschiebungen werden im Einklang mit Röntgenfluoreszenz- und Kernresonanzmessungen durch veränderte Valenzband-Zustandsdichten in den Legierungen interpretiert.

1. Introduction

Optical studies can give considerable information on the electronic structure of alloys. In the visible and near ultraviolet, however, the measured spectra contain information on both filled and empty electronic states, and it is difficult to separate them, especially if the measurements precede all quantitative theoretical work on the electronic structure of the alloy. The use of optical transitions from core levels, as in far ultraviolet and soft x-ray absorption spectroscopy, gives promise of revealing structure only due to the final states, the empty states above the Fermi level.

In this paper we report absorption data on alloys of Al with the 3d transition metals V, Fe, and Ni, and with Cu and Pr. In all cases there are transitions from p-like core levels (also 4d for Pr) within the energy range, 30 - 150 eV studied here. The continuous spectrum of synchrotron radiation [1] was used for the measurements, which means that no structure of significant size was missed. Since there exists no general theory of alloys, it is not always clear what will be the best way to begin to describe the electronic structure of a given system. Six of the alloys studied are ordered, which makes the notion of band structure a well-defined concept, and the effect of ordering can be seen in the results of our measurements. For the disordered alloys, which are by no means dilute, a model to describe the electronic structure must be very simple and provisional.

The Al $L_{2,3}$ edge at 72.6 eV has been studied extensively [2,3]. At the onset of the absorption there is a "spike" which has been attributed to a many-body-effect [2-4]. At slightly higher energies there is a region of absorption whose atomic origin is 2p-ns. It is not quite clear [5,6] whether structure in this region due to the density of final states is present in Al with-

out impurities, so solid state effects in the alloys may prove difficult to see. At still higher energies (7-10) transitions derived from atomic 2p-nd transitions occur, delayed in strength above the onset by the effect of the centripetal barrier on the matrix element of absorption (11). This gives rise to a large, broad peak, modified in the crystalline state. This modification has been interpreted (12) as extended x-ray absorption fine structure (EXAFS) (13), caused by the backscattering of the outgoing electron wave function by the neighboring atoms, whose kind and location is changed upon alloying. Recently evidence for the EXAFS origin of this structure was given by its disappearence on melting (14).

The $M_{2,3}$ transitions of transition metals (15) and the $N_{4,5}$ transitions of Pr (16) have been studied previously in pure metals. In all cases, there is no resemblance of the spectra to the expected density of states above the Fermi energy. This was attributed to the exchange interaction of the excited electron with the remaining hole (atomic multiplet splitting) and was calculated in detail for the $N_{4,5}$-transitions of the rare earths (17). For the lighter transition metals preliminary results of calculations on the $M_{2,3}$ transitions (18,19) along the lines successful for the rare earths show that the edge can be distorted severely from that for a one-electron atomic calculation. The exchange splitting of a multiplet cannot explain the $M_{2,3}$ absorption of Cu, which has a filled 3d shell, nor of Ni, which has a filled 3d shell after absorption. Yet the absorption of these metals near threshold is not one-electron like. For Ni it has been proposed recently (20) that the shape of the absorption peak was due to the interaction of an exciton line with an underlying continuum. The starting point for understanding all these transitions is atomic in origin, which means that localization of the states has to be presumed. The degree of localization can be tested by the effect of alloying as seen in the absorption spectra. Up to date only few results on absorption measurements of alloys in this energy range have been reported (21-25).

In the following we describe the methods of sample preparation and measurements (section 2), both of which differ from the more conventional methods. We can compare directly the spectra of the alloys with those expected from a superposition of spectra of the components, and with spectra of only one of the components. The results over the full range 30 to 150 eV (20 to 150 eV for Pr and $PrAl_2$) are presented in section 3. In section 4 we compare the pure metal and the alloy spectra with other absorption measurements when available and correlate the position of the Al $L_{2,3}$ edge with soft x-ray emission data. The results are discussed in section 5. A discussion of the structures observed in the energy region a few eV above the Al $L_{2,3}$ edge is not considered here since it was published previously [25]. These structures were interpreted as a density of states effect in the case of NiAl and FeAl with the help of a band structure calculation [26]. Because of the presence of these strong band-structure features in the vicinity of the edge, we abstain from discussing possible connections of the Al $L_{2,3}$ edge shape in these alloys with the many-body edge theory [4]. Already in pure Al the so called "spike" at the edge [2,3] is only a tiny peak which cannot be unambiguously distinguished from a density of states feature.

2. Experimental Method

2.1 Film preparation

Because of the generally large absorption coefficients in the spectral region investigated the film thickness ranged from 100 Å to 1000 Å. Films of pure transition metals thicker than about 600 Å and alloy films thicker than about 1000 Å could not be prepared successfully. Internal stresses [27] caused them to break and to coil. The films were prepared by vacuum evaporation (pressure $\approx 5 \times 10^{-7}$ Torr during evaporation). Copper mesh (hole separation 34 µm, 75 % transmissivity) was smeared with a solution of 2.5 % collodion in amylacetate, which after drying forms a thin continuous substrate. It was found

that collodion films that were too thick were destroyed during evaporation of carbon (see below) and could not be dissolved. The evaporant was condensed onto this substrate and after film preparation the collodion was dissolved thoroughly.

The constituents of an alloy were simultaneously evaporated from two independent sources. In case of the transition metal alloys Al was evaporated from a special resistance heated boat and the non-Al component from a 10 kW electron gun. In case of $CuAl_2$ and $PrAl_2$, Cu and Pr were evaporated from a boat and Al from the electron gun.

The rate of evaporation, ranging from 30 to 150 Å/sec, and the thickness were measured by quartz crystal monitors for each of the two metals separately and were recorded automatically. The evaporation rate of the component evaporated from the boat was stabilized by closed loop control, while that of the electron gun proved to be sufficiently constant without feedback. The rates were adjusted before the substrate was exposed to the sources. If the evaporation rate of either constituent deviated by more than 5 % from its face value at one instant during the film preparation, the film was rejected. The quartz monitors were calibrated with thicker films, ≈ 2800 Å, whose thickness was measured by the Tolansky method with an estimated accuracy of 1.5 %. The crystal structures [28], which are listed in Table 1, and the correct compositions [29] of the alloys were confirmed by electron diffraction measurements on films prepared simultaneously with those used for the optical measurements. No phases except the main phase were detected in any case.

Since all the components are to some extent reactive with oxygen, a 50 Å layer of carbon was evaporated before and after the evaporation of the alloy without breaking the vacuum, using another hearth of the electron gun. This served to mechanical support the thin films as well as to protect the reactive films

from the air and from the solvent for the collodion. Pr is the most easily oxidized metal we used and is a good test of the efficacy of the protective layers. Figure 1 shows the transmission of films of Pr with and without the carbon layers. The fine structure is seen to be different for the pure and the oxidized metal. This is in disagreement with the statements in Ref. [16]. The difference between the spectra of metallic Pr and Praseodymium oxid has been confirmed recently [30] by means of yield spectroscopy at UHV-conditions. This proves that results published previously on Pr oxide [31] were related to structure from the oxide.

In addition to alloy films, sandwich films were prepared in which the two constituents were evaporated one after the other with a layer of carbon between them to prevent interdiffusion. Films of the transition metals, of Cu, and of Pr with carbon, and films just of 100 Å carbon were also evaporated. These were useful in our two-beam spectrometer as reference foils (see below).

After preparation the alloy films were annealed for 90 min at 250° C at a pressure of 1×10^{-7} Torr. Test spectra revealed increased sharpness of the absorption edge with increased annealing. The above conditions produced edges as sharp as those after further annealing. More details are given elsewhere [32].

2.2 Optical measurements

The continuous spectrum of synchrotron radiation from the synchrotron DESY was used [1], after passage through a monochromator [33] specially designed for synchrotron radiation. The range from 21 to 150 eV could be covered with a resolution of about 1:500. Stray light and higher-order diffracted light presented no problems. The wavelength calibration in the region of the L_1 and $L_{2,3}$ structures of Al [10,34] was sufficiently good that only negligible errors occured from the calibration.

A recently-described two-beam densitometer was installed behind the exit slit [35,36]. The radiation is reflected at 4° from grazing incidence from a rotating mirror which sends the light alternately through two samples to separate detectors, electron multipliers with KCl coated cathodes. If T_1 and T_2 are the transmissions of the two films, $\gamma(T_1/T_2)$ can be recorded, where γ is a correction factor for differences in the detector's and the mirror's reflections. γ can be measured by leaving both sample positions empty; γ is only very little dependent on photon energy in the whole spectral range investigated [36].

Several possibilities are available for measurements:

1. If sample 1 (transmittance T_1) is a pure metal or an alloy film with its carbon protective layers and sample 2 (transmittance T_2) is a carbon film, $T(E) = \gamma \cdot T_1(E)/T_2(E)$ and γ are measured and can be processed to yield the absorption coefficient of the metal or alloy, free of the effects of the carbon. This is

$$\mu(E) = -\frac{1}{D} \ln (T(E)/\gamma) \qquad (1)$$

where D is the film thickness and E the photon energy.

2. The change in the absorption coefficient of Al upon alloying can be measured directly if sample 2 is the alloy film of thickness D_L and sample 1 is a pure metal film of the other constituent M. Its thickness D_M was chosen to be the thickness of a film with the same amount of M per unit area as it is in the alloy film. Correspondingly the equivalent thickness of the Al in the alloy is D_{Al}. From the directly-measured quantity $T = \gamma(T_M/T_L)$ one gets an effective absorption coefficient

$$\mu^*(E) = \frac{1}{D_{Al}} \ln(T(E)/\gamma) = \frac{1}{D_{Al}} (\mu_L D_L - \mu_M D_M) \qquad (2)$$

The absorption of metal M is eliminated if its spectral shape and absolute value per contributing atom is not changing in the alloy. The contribution to the absorption of the Al in the alloy is displayed more prominently.

A test of this method was performed by measuring the well-known absorption of Al [7-10] both from direct transmission spectra according to Eq. 1 and from quotient spectra according to Eq. 2. In the latter case sample 2 was a sandwich film using V, Fe, Ni, and Cu for M. In these cases μ^* should be equal to the absorption coefficient for pure Al, which, in fact, turned out to be the case within ±5 % in the whole spectral range (Fig. 2). This agreement demonstrates the ability of our measuring methods and the accuracy with which film thicknesses were controlled.

3. In order to determine more exactly the shift of the Al $L_{2,3}$ edge, sample 1 can be a sandwich film and sample 2 the alloy. These spectra are best understood in conjunction with the spectra of μ for both the alloy and Al. Figure 3 shows the result of such a measurement (dashed dotted curve) for an alloy of 16 atomic % Al in V. From A to B the absorption edge of the alloy determines the slope, from B to C the edge of pure Al in the sandwich appears with reversed sign, and finally, the continuation of the rising Al edge of the alloy is observed from C to D.

The dashed curve, taken by method 1, has the Al edge superimposed on the rapidly falling absorption of V, while in the spectrum taken by method 2 (solid curve) the edge shows up clearly, but the accuracy with which small shifts with respect to that of pure Al can be determined depends on the reproducibility of the wavelength drive of the monochromator.

The processing of about 200 spectra was carried out with the aid of an "on-line" data processing system [37]. The errors in the absolute value of the absorption coefficient above 70 eV are on the average about ±5 % and result primarily from uncertainties in the film thickness and slow temporal changes in the relative sensitivities of the two detectors. The latter effect was reduced to about ±3 % by calibrating various measured spectra with that of a single alloy film remeasured again and again over the course of the entire series of measurements. The relative shapes of the spectra over an energy interval of some 10 eV could be determined essentially errorfree because of the double-beam system and the continuous spectrum of synchrotron radiation.

In the 30 - 60 eV region the errors in the absolute value of μ rise to about ±15 % and those in μ^* to about ±30 % because here small amounts of Al_2O_3, incorporated during the evaporation, give large effects. The absorption coefficient of Al_2O_3 at 30 eV is 8.6 x 10^5 cm^{-1} (36,38) comparable to that of the alloy constituents M. Moreover the absorption coefficient of carbon rises to about 5 x 10^5 cm^{-1} in this region (39). Small differences in the thicknesses of the protective layers and the reference carbon film can have large effects in this spectral region. Inconsistencies between absolute values of μ and μ^* in Figs. 4-8 arise from such errors.

Fig. 2 and Figs. 4-8 show spectra of μ and μ^* for all the alloys measured and for the individual component metals. The structures in μ^* at the Al $L_{2,3}$ edge have been presented in more detail in another publication (25). The percentages listed are the aluminum content of the alloys in atomic percent. For V and the V-alloys absolute values of μ and μ^* are not given because the results were obtained on only one film of each composition. The scale for these spectra (Fig. 4) is approximately 10^5 cm^{-1} per unit for both μ and μ^*.

3. Results

3.1 Transition metals and transition metal-Al alloys (Figs. 4-6,9)

3.1.1 30 - 70 eV region

The structure in the low energy region is due to the excitation of the 3p ($M_{2,3}$) levels of the transition metals. In this region the influence of alloying can be seen more clearly in the spectra of μ^*. The Al gives only a weak, structureless background, so that the spectrum of μ^* is a difference spectrum, showing the change in the absorption of the transition metal brought about by the addition of Al.

For V and Fe alloys the energy of the onset of the $M_{2,3}$ absorption is the same as in the pure metals. In NiAl and $NiAl_3$ the onset shifts by 1.3 eV and 2.1 eV to higher energy, respectively (see Fig. 9 and Table 2). The broad maximum above the onset shifts to higher energy upon the addition of Al to V and to Fe. The structures in the μ^* spectra of these alloys reflect the changes of the shape of this

maximum. For VAl_3 and V-Al (41 %) the step between 36.5 and 39 eV for pure V in the μ spectrum has disappeared almost completely, while it is present, but weaker, in the μ spectrum of V-Al (28 %). This leads to a maximum in the μ^* spectrum (Fig. 4b) at 38.8 eV. For VAl_3 and V-Al (28 %) the $M_{2,3}$ absorption edge begins with the same slope as that of V, while the slope before the edge for V-Al (41 %) is steeper, causing the drop in the μ^* spectrum between 34.0 and 36.4 eV. At 44 eV a shoulder occurs in the spectra of both alloys, which appears as a minimum in μ^* at this energy.

In the Fe-Al alloys the onset of absorption between 51.9 and 52.2 eV is steeper than in pure Fe, which is easily seen as a peak in the μ^* spectra (Fig. 5b). The step at 62.5 eV in pure Fe does not occur in the alloys. The μ spectrum of Fe-Al (11 %) is not shown in Fig. 5a, because it is practically identical to that for pure Fe due to the small Al-content and the relatively strong absorption of Fe.

3.1.2 Al $L_{2,3}$ edge

The pronounced increase in μ at the Al $L_{2,3}$ edge remains recognizable in all the spectra. The changes of this edge were discussed and displayed in Ref. [25] (see especially Figs. 1 and 2 therein). Table 1 gives the energies of the onset of the Al $L_{2,3}$ edge for each alloy studied. The edge is steeper for the ordered alloys than for the disordered alloys.

The shapes of the spectra above the edge fall into two classes. For NiAl, FeAl, and V-Al (28 %) maxima occur, clearly separated from the top of the $L_{2,3}$ edge by about 2 eV. These maxima are especially sharp for NiAl and FeAl and have successfully been interpreted as a band-structure feature [25]. The maxima for $NiAl_3$ and for the V-alloys are broader, less prominent, and are closer to the $L_{2,3}$ edge. The spectrum of Fe-Al (11 %) falls between these two classes.

3.1.3 Above 80 eV

Here the μ^* spectra are essentially those of the Al L-absorption in the alloys, with the transition metal $M_{2,3}$-absorption eliminated. The large maximum at 97 eV

for Al is evident in all the alloy spectra (Figs. 4b - 6b). The energy of the peak is not noticably changed. The absolute values of μ^* at the maximum vary between 7.1 (for NiAl) and 2.3 x 10^5 cm^{-1} (for Fe-Al (11 %)). The value is 4.2 x 10^5 cm^{-1} for pure Al. The subsequent minimum in the Al spectrum is changed for all alloys. The pronounced decrease of the absorption at energies above the peak is strongly reduced with the alloys. There are significant changes in the region of the L_1 absorption at 117 eV. For $NiAl_3$ and the V alloys, a simple edge occurs instead of the more complicated structure found with pure Al.

3.2 Cu and $CuAl_2$ (Fig. 7)

For both pure Cu and $CuAl_2$ the $M_{2,3}$ absorption begins at 73.6 eV. Because of the overlap with the Al $L_{2,3}$ absorption, this cannot be seen directly in the μ spectrum. A shift of the $M_{2,3}$ edge would appear in the μ^* spectrum as a marked oscillation, as in the case of NiAl, but non occurs for $CuAl_2$ (Fig. 7b). Directly beyond the onset of the Al $L_{2,3}$ absorption there is a sharp maximum. The L absorption above 80 eV is similar to that in the transition metal alloys.

3.3 Pr and $PrAl_2$ (Fig. 8)

The Al L-absorption for $PrAl_2$ is similar to that for the transition metal alloys. The Pr structure between 105 and 150 eV is unchanged upon going from Pr to $PrAl_2$, except for a small change in the decrease above the principal maximum. In the μ^* spectrum, the sharp Pr structures cancel out. The maximum at 25 eV does not change its position, but it becomes stronger in the alloy, so that a weak maximum remains in the μ^* spectrum.

4. Comparison with other measurements

The overall appearance of our spectra for the pure metals agrees well with the spectra reported by other authors [7-10,15,16,23,40]. Characteristic features of our spectra for the transition metals and Cu are given in Table 2 along with results form Ref. [15]. Deviations in details which are not important for the following discussion will not be described. The absorption coefficient obtained by optical measurements of Pr between 21 and 90 eV has not been published previously, while

our data in the region of the 4d fine structure have been compared above (Fig. 1) with those of Ref. [16].

Yamaguchi et al. [21] have measured transmission spectra of Al-rich alloys with Ti, V, Mn and Ni, not exceeding about 20 at. % of the transition metal. These samples were in a different composition range from ours, and probably had different crystal structures. (Yamaguchi et al. did not determine the structure of their films.) In the Al-rich region the crystal structures of the Al-transition metal alloys are sensitive to the preparation conditions and to the exact composition [29]. For some of the measurements in Ref. [21] it is likely that several phases were present. Nevertheless, there are some similarities with our spectra for lower Al-concentrations: broadening of the Al $L_{2,3}$ edge, additional absorption peaks, at most 2 eV wide, lying between 0.6 and 1.5 eV above the $L_{2,3}$ edge, and deformation of the minimum following the dominant 97 eV absorption maximum.

The position of the core level relative to the Fermi level can also be obtained from x-ray emission spectra. The $L_{2,3}$ emission bands of Al in alloys with transition metals have been investigated by Watson et al. [41]. In Table I we show their results for the position and width of the edge, for comparison with the results of our absorption measurements. The agreement is generally good. The emission data show a tendency to greater shifts. For V-Al (16 %), Fe-Al (11 %) and FeAl, the width of the absorption edges cannot be determined unambiguously because it is difficult to separate it from structures at higher energy (see Ref. [25]). Therefore two values for the width of these edges are given in Table I. The discrepancy between the results for NiAl may be the result of better sample quality for the absorption measurements, for we take a sharper edge as an indication of higher crystalline order.

5. Discussion

5.1 General

The general appearance of the alloy spectra differs distinctly from that of a

superposition of the spectra of the components. This need not always be the case, see e.g., Cu-Ni [23]: The L absorption of Al is changed more than the M absorption of the transition metals or Cu. A complete understanding of the spectra we have measured is clearly not possible at this time. In the following we discuss several points that connect with our present ideas about these alloys and the optical transitions under consideration.

5.2 The Al L absorption above the edge

An atomic calculation of the absorption spectrum of the 2p electrons in Al gives only one large broad peak around 95 eV [42]. It arises from the dipole matrix element and is essentially a delayed 2p - nd absorption. The modulation of the cross section is believed to be a solid state effect [12,14], and a recent explorative calculation [12] shows that this is probably the result of the backscattering of the outgoing electrons from the atoms in several neighboring shells (EXAFS [13]). Upon alloying these neighbors become different types of atoms, occur at different locations if the crystal structure changes, and, for disordered alloys, different Al sites may have different relative numbers of neighbors of each type. The latter should wash out this structure to some extent for disordered alloys, while the former two effects should produce changes, but not necessarily diminished structure. This is qualitatively what was observed, although no significant shift of the most prominents peak in the Al spectrum at 97 eV occurs and wash-out rather than a shifting of structures is the rule.

5.3 Shift of the edges

The Al $L_{2,3}$ edges shift from their positions in pure Al, both to lower and higher energy, depending on the transition metal. For V-Al the shifts increase with increasing V concentration. The shifts are negative upon the addition of V, and positive for Cu, with a monotonic dependence on the position of the transition metal in the periodic table. These shifts could arise from shifts in the Fermi level, charge transfer to or from the Al atom, or from a change in the effective radius of the Al valence electron distribution. It was originally hoped

that the measurement of these shifts on a series of alloys with different transition metals would allow to estimate which effect dominates, but it appears that more than one effect is important and no separation can be effected. For example, if charge transfer were to dominate, all the shifts for the transition metals should be positive, since Al is more electropositive than anyone of them (43). Clearly the shift of the Fermi level and of the valence wave functions must also be considered in order to obtain the negative shifts for these metals.

Charge transfer should play only a small role in the V-Al system for the electronegativity difference is small. Van Ostenburg et al. (44) conclude from their Knight shift measurements that the s and p electrons tend to go into states in the lower part of the valence band upon alloying with V. In agreement with this, Watson et al. (41) find a strong increase in the intensity of Al $L_{2,3}$ emission from the lower part of the valence band with respect to that from the higher part, as Al is added to V. The shift of the Al $L_{2,3}$ edge to smaller energy in the V-Al alloys means that the s-p density of states for Al increases in the lower part of the valence band, moving the Fermi level to lower energy. This density of states increase grows with increasing V concentration, the maximum shift of both the Fermi level and the Al $L_{2,3}$ edge occuring for V-Al (16 %). Note that the emission and absorption spectra show no discontinuity of the shift for the ordered alloy VAl_3.

For NiAl and $NiAl_3$ Bradley and Taylor (45) have determined an extremely short bond length between the Al and Ni. This means there is considerable overlap of the Ni and Al valence electron wave functions, leading to the ordered lattice. It is very likely that Ni has a filled 3d shell. Three valence electrons per unit cell is the upper limit for stability of the CsCl structure (46) and Al already contributes the 3. The remaining 10 electrons per cell must go in the 3d band. This picture is made more plausible by the fact that if more than 50 % Al is present, vacancies occur on the Ni sites (45). Also measurements of x-ray emission relative intensities (47) give evidence for the filling of the Ni d-shell. The strong mixing

of Ni and Al valence wave functions then occurs primarily for states below the Fermi level. This is reinforced by the observation that the Ni $M_{2,3}$ edge is reduced by a factor of 1/5 in NiAl with respect to that of a layer of Ni with the same equivalent thickness of Ni atoms. It also explains the large shift of the Ni $M_{2,3}$ edge with the addition of Al - the Fermi level shifts rapidly higher because it lies above the Ni d band in a region of small, free-electron-like density of states. Seitchick and Walmsley (48) concluded from Knight shift and electronic specific heat data that the Al wave function in NiAl had very little s-character at the Fermi level and that the density of states is small there. The reduction in height of about 1/3 of the Al $L_{2,3}$ edge in NiAl with respect to that in Al is a consequence of this small density of empty s-like states at the Fermi level.

In contrast to NiAl, Fe-Al (11 %) and Fe-Al are ferromagnetic, thus it is concluded that, with those alloys the Fe 3d shell is not filled. Wenger et al. (45) have determined that there are 7.8 d-electrons below the Fermi level in FeAl. As a consequence the $M_{2,3}$ edge is pinned to a region of high d state density and does not shift. The shift of the Al $L_{2,3}$ edge to smaller energies for these two alloys can be explained in the same way as for V-Al alloys, as the result of an increased density of Al conduction band states below the Fermi level upon alloying with Fe. The Al $L_{2,3}$ edge is not so well defined for FeAl as for NiAl. The degree of order in the former seems to be smaller. This can be guessed from the phase diagram, in which 50 % Al - 50 % Fe does not coincide with a maximum in the melting point (29).

For $CuAl_2$ the Al $L_{2,3}$ edge shifts to higher energy, as for $AuAl_2$ (22). For both alloys, the noble metal has the higher electronegativity. Pr has a lower electronegativity than Al, and the Al $L_{2,3}$ edge shifts to lower energy in $PrAl_2$. With these three alloys charge transfer appears to provide the dominant influence for the edge shift.

5.4 Absorption maxima of transition metals, Pr and their alloys

The fact that the $M_{2,3}$ absorption maxima below 70 eV for the V and Fe alloys are essentially unchanged from those in the pure transition metals is an indication of the localized (atomic) nature of these transitions [17-19]. The same holds for the large peak at 25 eV in the spectra of Pr and $PrAl_2$, which is shaped by a collective atomic resonance in the 5p - 5d transitions [49].

The fine structure at the onset of the 4d - 4f transitions of Pr (Fig. 1) is practically the same in both Pr metal and $PrAl_2$, while the oxide shows considerable differences. Recently also spectra of PrF_3 became available [50]. The fine structure for PrF_3 is practically the same as that for the oxide. The differences between metal and alloy on the one side and the salts on the other side is an indication for the influence of the metal electrons on the empty f-states. A more than qualitative understanding of these differences will need however some effort on the theoretical side, probably a combination of atomic calculations like those of Dehmer et al. [17] with solid state calculations. This holds quite generally for several of the results found in the course of this investigation. While theory, especially with respect to alloys, is not yet very elaborate, absorption structures can now quite readily be investigated with the experimental methods described here.

Acknowledgement

We wish to thank D.W. Lynch for his help in preparing this manuscript and for several useful discussions.

References

+ now at Philips Forschungslaboratorium Aachen, 5100 Aachen, W.-Germany

++ now at IBM Thomas J. Watson Research Center, Yorktown Heights, N.Y. 10598

1. R.P. Godwin, in: Springer Tracts in Modern Physics, Vol. 51 (Springer Verlag, Berlin 1969); F.C. Brown, in: Solid State Physics, Vol. 29 (Academic Press, New York, London 1974); C. Kunz, in: Vacuum Ultraviolet Radiation Physics, E.E. Koch, R. Haensel, C. Kunz, Eds. (Pergamon/Vieweg, Braunschweig 1974) p. 753
2. C. Kunz, R. Haensel, G. Keitel, P. Schreiber and B. Sonntag, in: Electronic Density of States. L.H. Bennett Ed. (NBS Special Pupl. 323, Washington 1971), p. 275
3. C. Gähwiller and F.C. Brown, Phys.Rev. B 2, 1918 (1970)
4. G.D. Mahan, in: Solid State Physics, Vol. 29, p. 75
5. A. Balzarotti, A. Bianconi, and E. Burattini, Phys.Rev. B9, 5003 (1974)
6. W. Gudat and C. Kunz, to be published
7. T. Sagawa, Y. Iguchi, M. Sasanuma, A. Ejiri, S. Fujiwara, M. Yokota, S. Yamaguchi, M. Nakamura, and T. Sasaki, J.Phys.Soc. Japan 21, 2602 (1966)
8. V.A. Fomichev, Sov.Phys. - Solid State 8, 2312 (1967)
9. R. Haensel, B. Sonntag, C. Kunz, and T. Sasaki, J.Appl.Phys. 40, 3046 (1969)
10. R. Haensel, G. Keitel, C. Kunz, P. Schreiber, and B. Sonntag, phys.stat.sol. (a) 2, 85 (1970)
11. U. Fano and J.W. Cooper, Rev.Mod.Phys. 40, 441 (1968)
12. J.J. Ritsko, S.E. Schnatterly, and P.C. Gibbons, Phys.Rev.Letters 32, 671 (1974)
13. see e.g. D.E. Sayers, E.A. Stern, and F.W. Lytle, Phys.Rev.Lett. 27, 1204 (1971)
14. H. Petersen and C. Kunz, Report DESY SR-75/04
15. B. Sonntag, R. Haensel, and C. Kunz, Sol. State Comm. 7, 597 (1969)
16. R. Haensel, P. Rabe, and B. Sonntag, Sol. State Comm. 8, 1845 (1970)
17. J.L. Dehmer, A.F. Starace, U. Fano, J. Sugar, and J.W. Cooper, Phys.Rev.Lett. 26, 1521 (1971); J. Sugar, Phys.Rev. B 5, 1785 (1972)
18. F. Combet Farnoux and M. Lamoureux, in: Vacuum Ultraviolet Radiation Physics E.E. Koch, R. Haensel, C. Kunz Eds. (Pergamon/Vieweg, Braunschweig 1974) p. 89
19. F. Combet Farnoux, in: Physica Fennica 9, Suppl. S1 p. 80, 1974
20. R.E. Dietz, E.G. McRae, Y. Yafet and C.W. Caldwell, Phys.Rev.Lett. 33, 1372 (1974)
21. S. Yamaguchi, S. Sato, E. Ishiguro, O. Aita, T. Hanyu, and H. Koike: Proc. of the III. Int. Conf. on VUV Radiation Physics (Ed. Y. Nakai, Tokyo 1971) 2a C 2-4
22. W. Gudat, J. Karlau and C. Kunz, Proc. Int. Symp. X-Ray Spectra and Electronic Structure of Matter, Vol. 1 (Ed. A. Faessler and G. Wiech, München 1973) p. 205
23. W. Gudat and C. Kunz, phys.stat.sol. (b) 52, 433 (1972)
24. J.H. Slowik, Phys.Rev. B 10, 416 (1974); J.H. Slowik and F.C. Brown, Phys.Rev.Lett. 29, 934 (1972)

25. H.-J. Hagemann, W. Gudat and C. Kunz, Sol.State Comm. 15, 655 (1974)
26. J.W.D. Connolly and K.H. Johnson, in: Electronic Density of States L.H. Bennett Ed. (NBS Spec. Publ. 323, Washington 1971) p. 19
27. L. Holland, Vacuum Deposition of Thin Films (Chapman and Hall Ltd., London 1963) p. 212
28. R.G.W. Wyckoff, Crystal Structures (Interscience Publ. New York 1965)
29. M. Hansen, Constitution of Binary Alloys (McGraw Hill, New York 1958)
30. W. Gudat and C. Kunz, unpublished
31. W. Gudat and C. Kunz, Phys.Rev.Lett. 29, 169 (1972)
32. H.-J. Hagemann, Internal Report DESY F41-74/4
33. H. Dietrich and C. Kunz, Rev.Sci.Instr. 43, 434 (1972)
34. K. Codling and R.P. Madden, Phys.Rev. 167, 587 (1968)
35. W. Gudat, J. Karlau and C. Kunz, Appl.Opt. 13, 1412 (1974)
36. H.-J. Hagemann, W. Gudat and C. Kunz, Report DESY SR-74/7 and J.Opt.Soc.Am. 65, 742 (1975)
37. U. Nielsen, Proc. Int. Symp. Synchrotron Radiation Users (Ed. G.V. Marr and I.H. Munro, Daresbury 1973) p. 13
38. G.H.C. Freeman, Brit. J. Appl. Phys. 16, 927 (1965)
39. M.W. Williams and E.T. Arakawa, J.Appl.Phys. 43, 3460 (1972)
40. F.C. Brown, C. Gähwiller and A.B. Kunz, Sol. State Comm. 9, 487 (1971)
41. L.M. Watson, Q.S. Kapoor, and D. Hart, Proc.Int.Symp. X-Ray Spectra and Electronic Structure of Matter, Vol. 2 (Ed. A. Faessler and G. Wiech, München 1973) p. 135
42. E.J. McGuire, Phys.Rev. 175, 20 (1968)
43. L. Pauling, The Nature of the Chemical Bond (Cornell University Press, Ithaca, 1960)
44. D.O. Van Ostenburg, D.J. Lamm, H.D. Trapp and D.W. Pracht, Phys.Rev. 135, A 455 (1964)
45. A.J. Bradley and A. Taylor, Proc.Roy.Soc. (London) A 159, 62 (1937)
46. L. Brewer, in: Phase Stability of Metals and Alloys (Ed. J. Stringer and R.I. Jaffee, McGraw Hill, New York, 1958) p. 39
47. A. Wenger, G. Bürri and S. Steinemann, Sol. State Comm. 9, 1125 (1971)
48. J.A. Seitchick and R.H. Walmsley, Phys.Rev. 137, A 143 (1965)
49. G. Wendin, private communication
50. D.W. Lynch and C.G. Olson, private communication

Table 1: Comparison of the shifts of the onset and the width of Al $L_{2,3}$ edge in alloys from absorption and x-ray emission (41) measurements. The width is defined as the energy difference between 10 % and 90 % of the height of the edge. In the first column the crystal structures of the alloys are given (ssl = solid solution).

Substance	crystal structure	shift of the onset of the Al-$L_{2,3}$ edge (eV)		Width (eV)	
		Abs. (±0.1 eV)	Emiss. (±0.05 eV)	Abs. (±0.1 eV)	Emiss. (±0.05 eV)
Al (position of onset)	fcc	72.6	72.76	0.15 (±0.02)	0.3
V-Al 16 %	bcc (ssl)	- 1.1	-1.25 (10 %)	1.8 (1,2)	0.85
V-Al 28 %	cubic (β-W)	- 1.1	-1.10 (24 %)	0.6	0.85
V-Al 41 %	bcc (ssl)	- 0.7	-0.95 (40 %)	0.9	0.9
VAl_3	tetrag. (Al_3Ti)	- 0.4	-0.65	0.7	0.94
Fe-Al 11 %	bcc (ssl)	- 1.0	-	2.5 (0.9)	-
FeAl	bcc (CsCl)	- 0.7	- 0.75	1.5 (0.8)	0.9
NiAl	bcc (CsCl)	- 0.3	- 0.55	0.15	0.55
$NiAl_3$	orthorhomb.	- 0.3	-	0.4	-
$CuAl_2$	tetrag. (Fe_2B)	+ 0.4	-	0.8	-
$PrAl_2$	cubic (Cu_2Mg)	- 0.6	-	0.2	-

Table 2: Characteristic values of the $M_{2,3}$ absorption maxima of transition metals and their Al alloys and of Cu.

E_1 Position of the onset of absorption
E_1' Position of the onset of absorption after Sonntag et al. (15)
E_2 Position of the principal maximum following the onset
E_2' Position of the maximum after Sonntag et al. (15)
$\Delta\mu$ Change of μ between E_1 and E_2,
$\Delta\mu'$ Change of μ between E_1' and E_2'

Element/ Alloy	E_1 (eV)	E_1' (eV)	E_2 (eV)	E_2' (eV)	$\Delta\mu$ (10^5 cm^{-1})	$\Delta\mu'$ (10^5 cm^{-1})
V	36.0	35.4	47.2	47.7	3.2	5.5
V-Al 16 %	-		49 ± 1		-	
V-Al 28 %	35.9±0.2		48 ± 1		3.0	
V-Al 41 %	36.0±0.1		47.5		1.7	
VAl_3	36.0		49.8		2.0	
Fe	52.0	51.7	56.2	57.1	6.4	7.2
Fe-Al 11 %	52.0±0.2		56.3		-	
FeAl	52.0		57.3		2.1	
Ni	64.2	63.9	67.9	68.5	3.8	3.7
NiAl	65.5		67.7		0.5	
$NiAl_3$	66.3		71.4		0.6	
Cu	73.6	73	80.1	79	1.2	0.5

Figure Captions

Fig. 1 Protection against oxidation, example: Pr. Upper curve: with carbon protective layers. Lower curve: unprotected foil which had been directly exposed to air; the additional structure originates from oxidation. Horizontal scale in all figures: photon energy.

Fig. 2 Absorption spectrum of Al: within the limits of experimental accuracy the same spectrum was obtained from direct transmission (μ) on single layer films and quotient (μ^*) spectra on sandwich films, see text and Eqs. 1, 2.

Fig. 3 Absorption of V-Al (16 %) alloy near Al $L_{2,3}$ edge. Dashed curve: absorption coefficient μ (Eq. 1), the Al edge is hidden by the rapidly falling V absorption. Solid curve: V absorption eliminated by measuring μ^* (Eq. 2). Dash-dotted curve: quotient spectrum of alloy and sandwich which directly displays the shift of the Al edge in the alloy.

Fig. 4 a) Absorption coefficient μ (Eq. 1) of V and V-alloys.
b) Relative absorption coefficient μ (Eq. 2). The zero lines of the spectra of V-Al 41 % and VAl_3 have been shifted as marked. In the region above the Al $L_{2,3}$ edge at 72.6 eV these spectra give essentially the absorption of Al in its alloy environments.

Fig. 5 Absorption coefficients μ and μ^* (Eqs. 1,2) of Fe and Fe-alloys. "x2" means that the μ values as read from the scale have to be multiplied by a factor of 2.

Fig. 6 Absorption coefficients μ and μ^* (Eqs. 1,2) of Ni and Ni-alloys.

Fig. 7 Absorption coefficients μ and μ^* (Eqs. 1,2) of Cu and $CuAl_2$.

Fig. 8 Absorption coefficients μ and μ^* (Eqs. 1,2) of Pr and $PrAl_2$.

Fig. 9 Absorption coefficient μ in the vicinity of the onset of the V, Fe, and Ni $M_{2,3}$ absorption of several alloys and the pure transition metals. The edges are normalized to equal height.

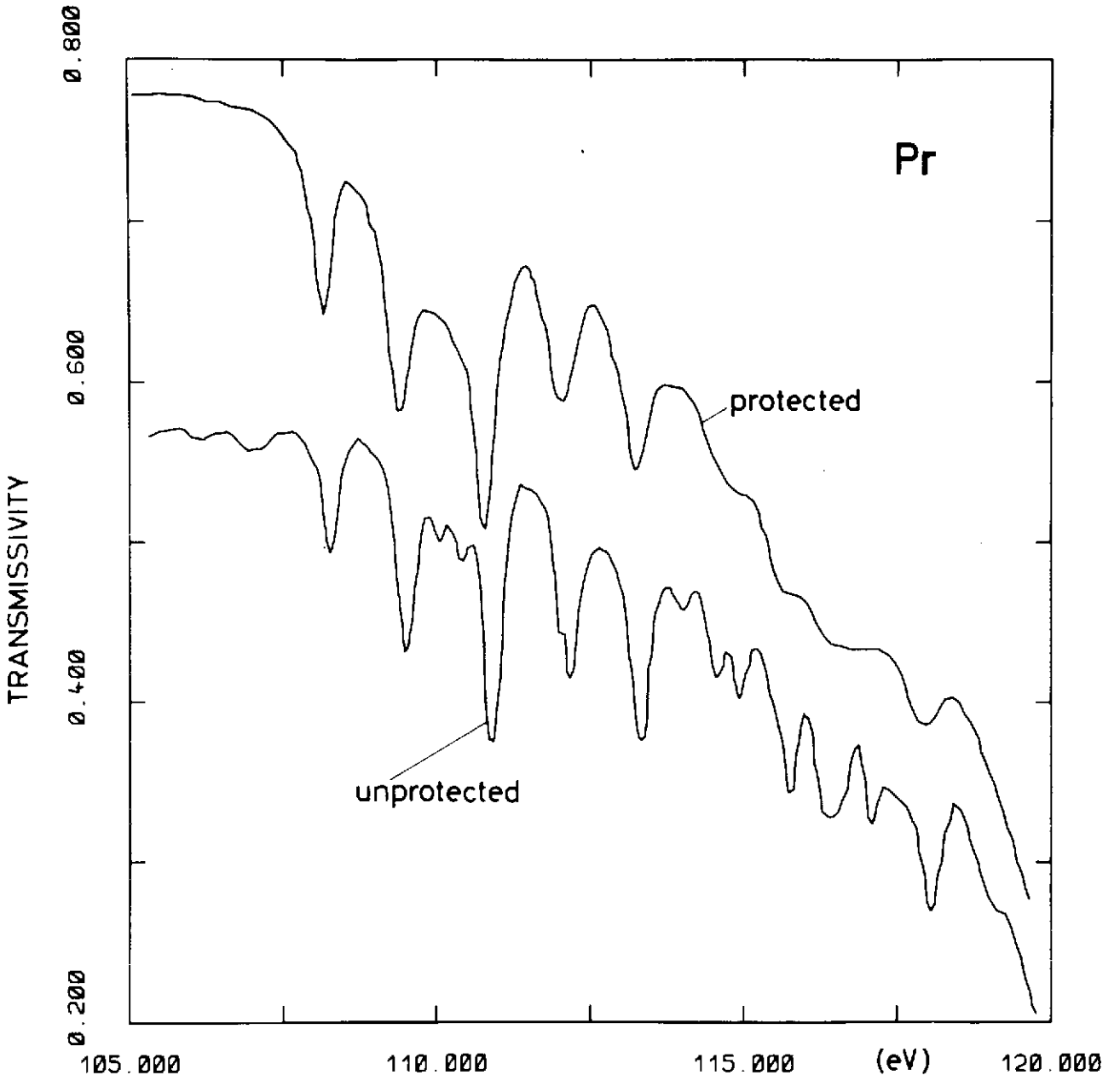
Pr
protected
unprotected
TRANSMISSIVITY
0.800
0.600
0.400
0.200
105.000
110.000
115.000
(eV)
120.000

Fig. 1

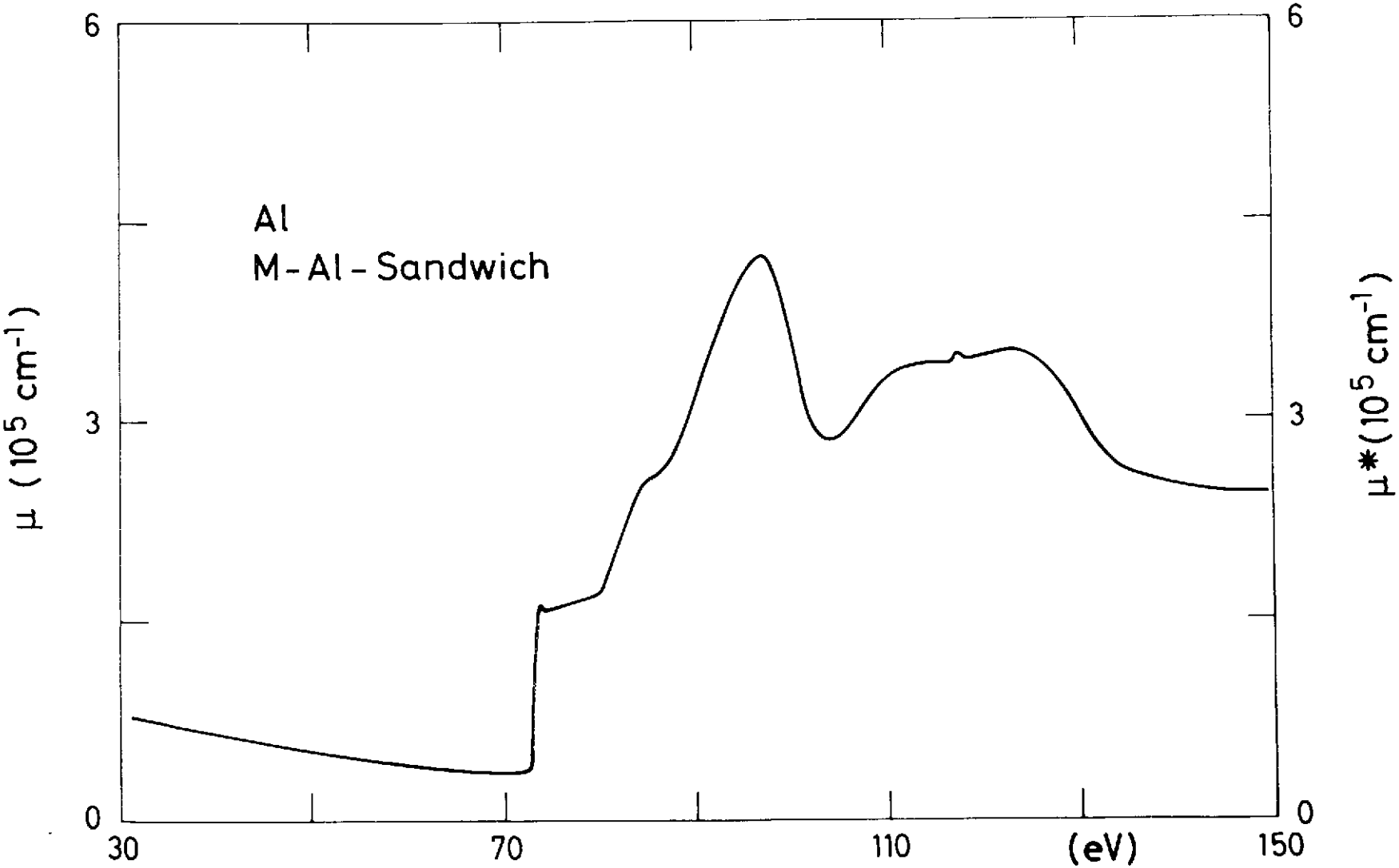

Fig. 2

arbitrary units
80
(eV)
75
70
V-Al, 16 %
A
B
C
D
absorption structures

Fig. 3

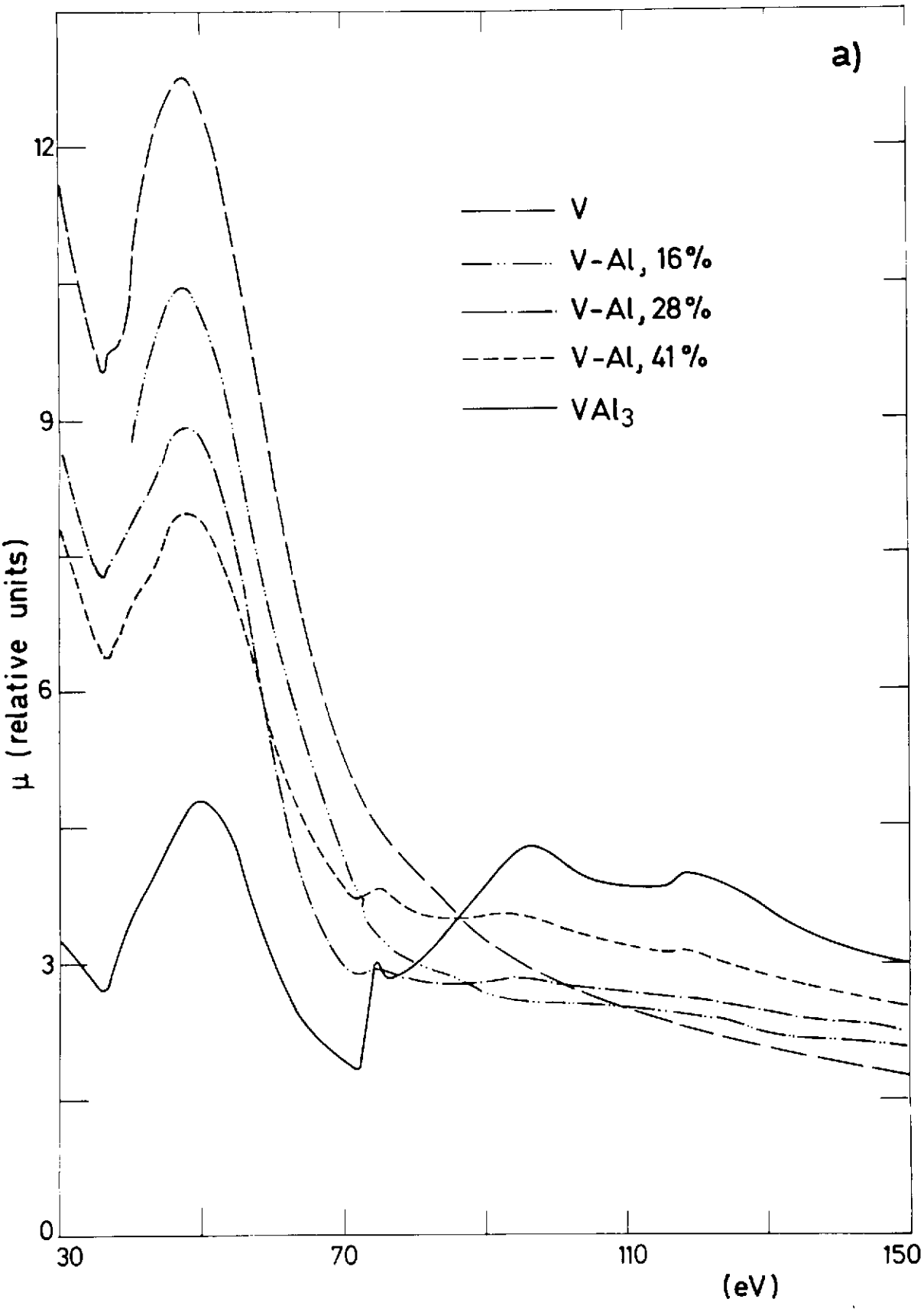
a)
V
V-Al, 16%
V-Al, 28%
V-Al, 41%
VAl3
μ (relative units)
0
3
6
9
12
30
70
110
150
(eV)

Fig. 4 a)

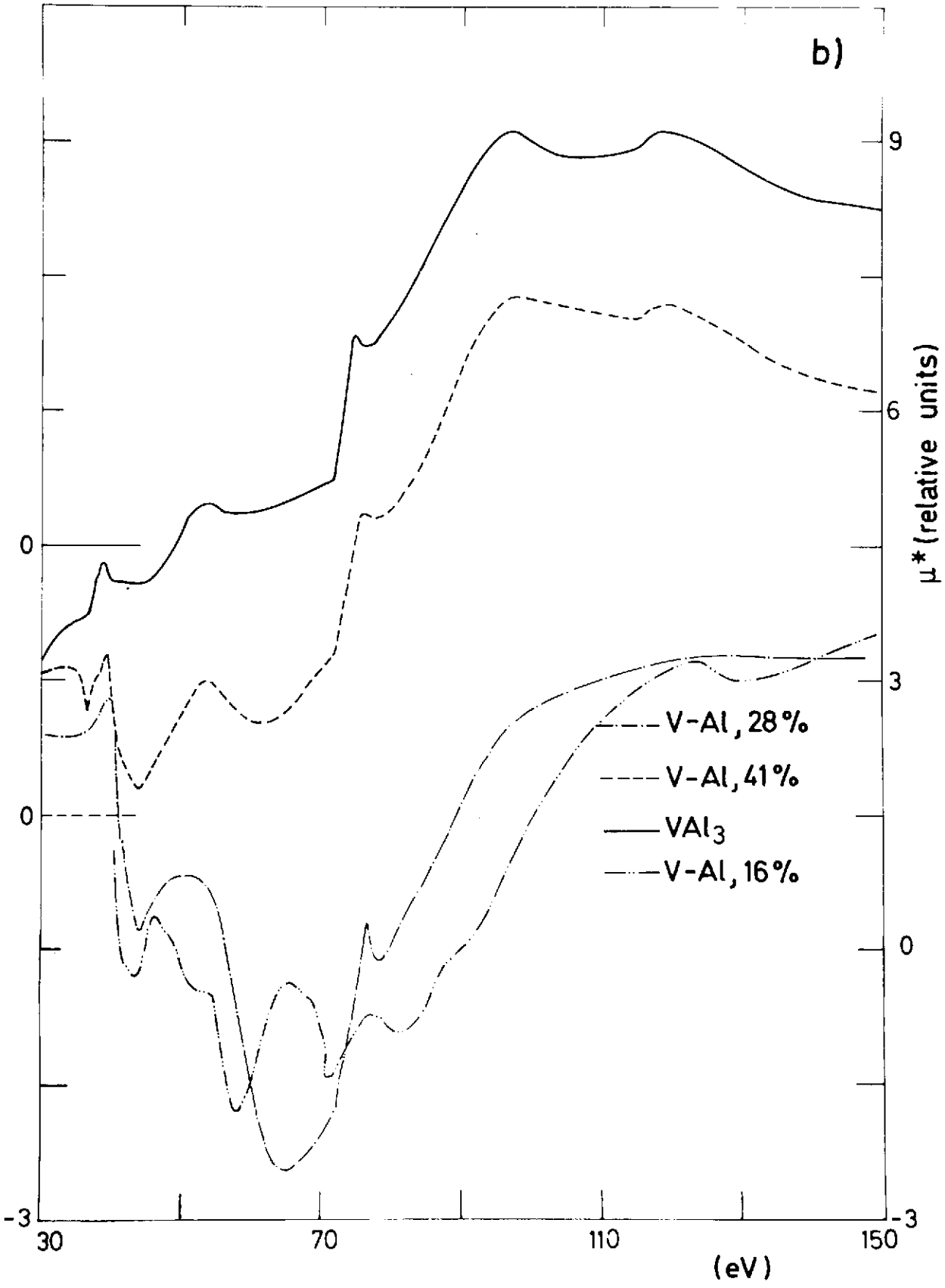
b)
9
6
3
0
-3
0
-3
30
70
110
150
(eV)
μ* (relative units)
V-Al, 28%
V-Al, 41%
VAl3
V-Al, 16%

Fig. 4 b)

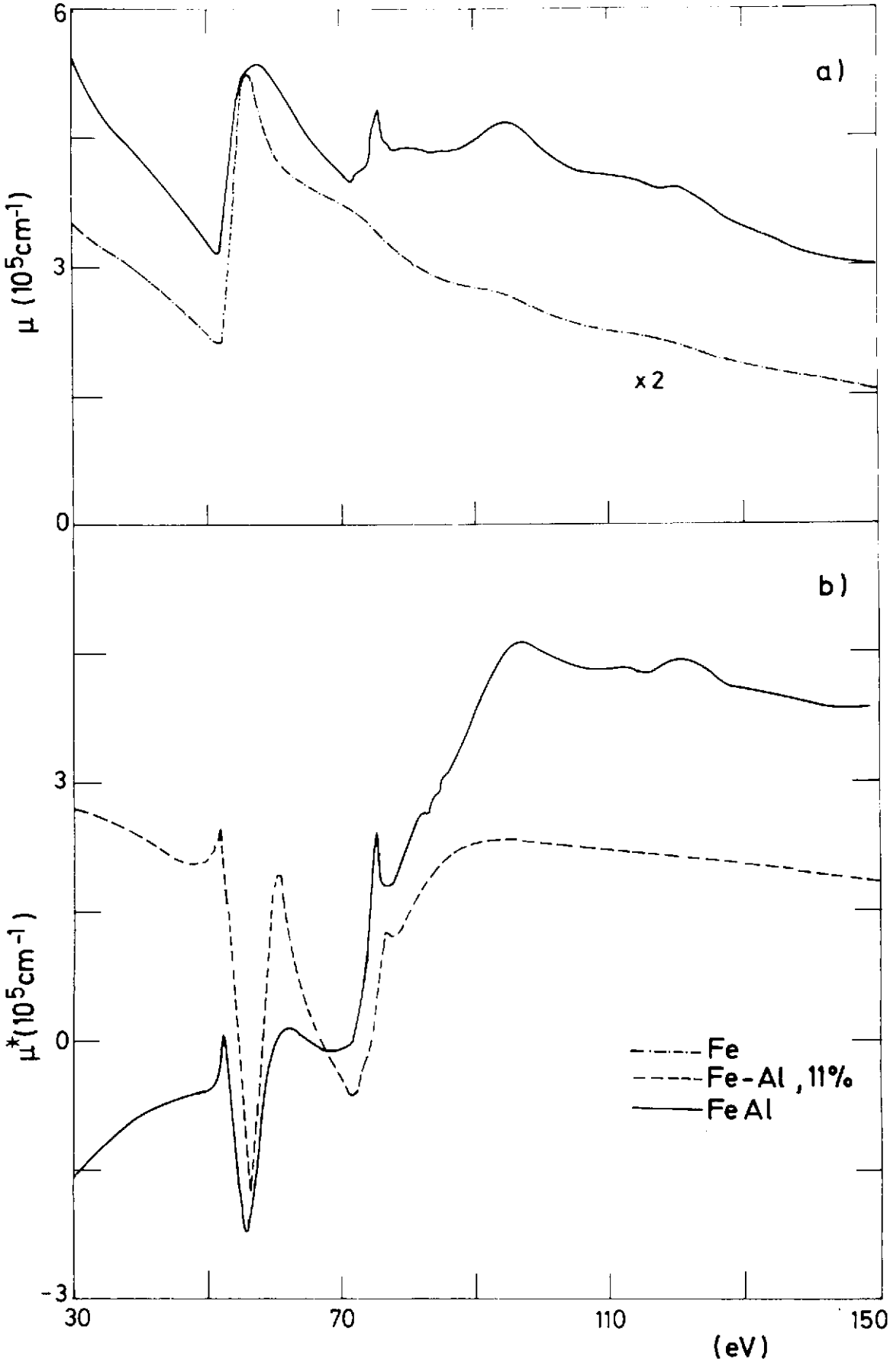

Fig. 5

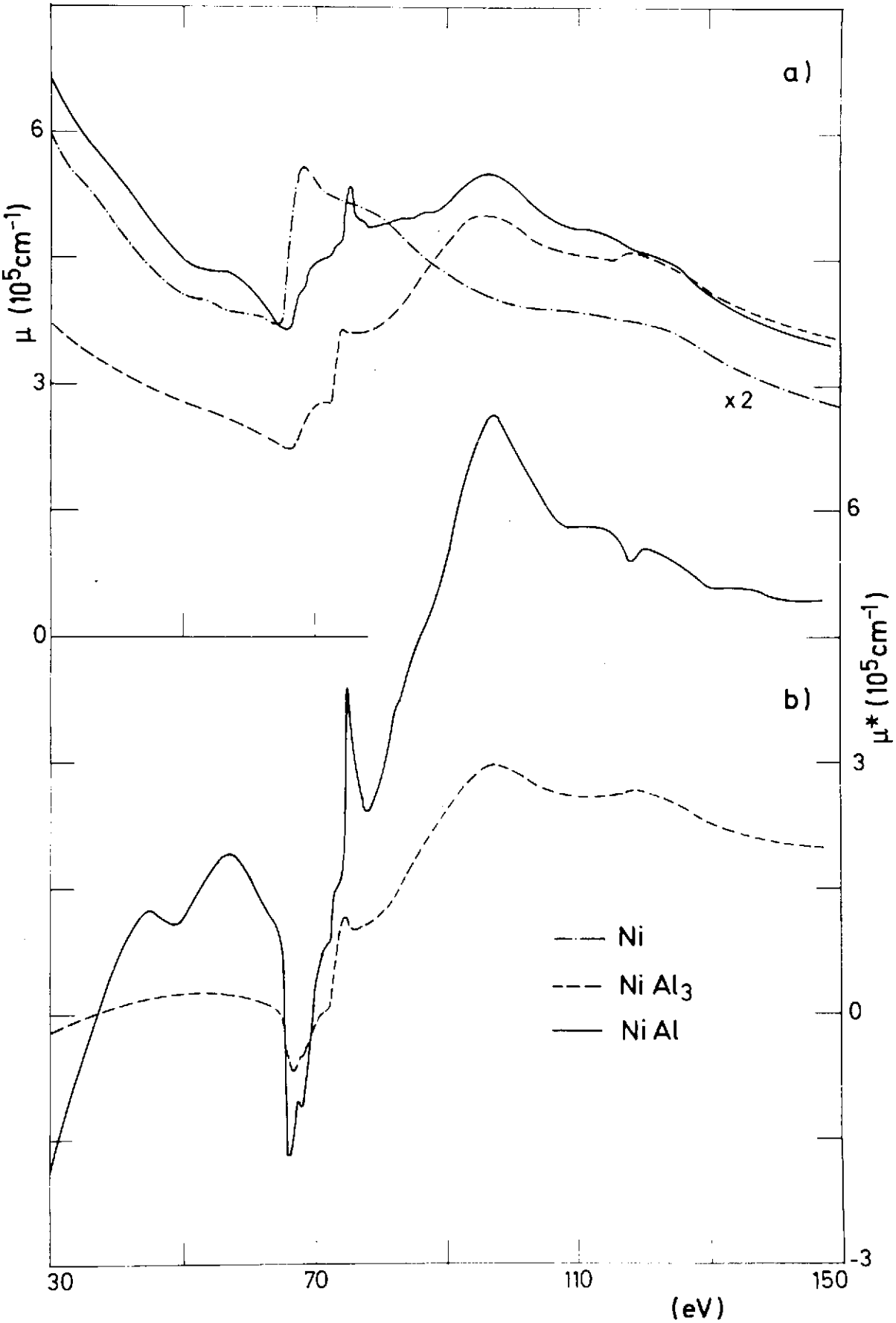

Fig. 6

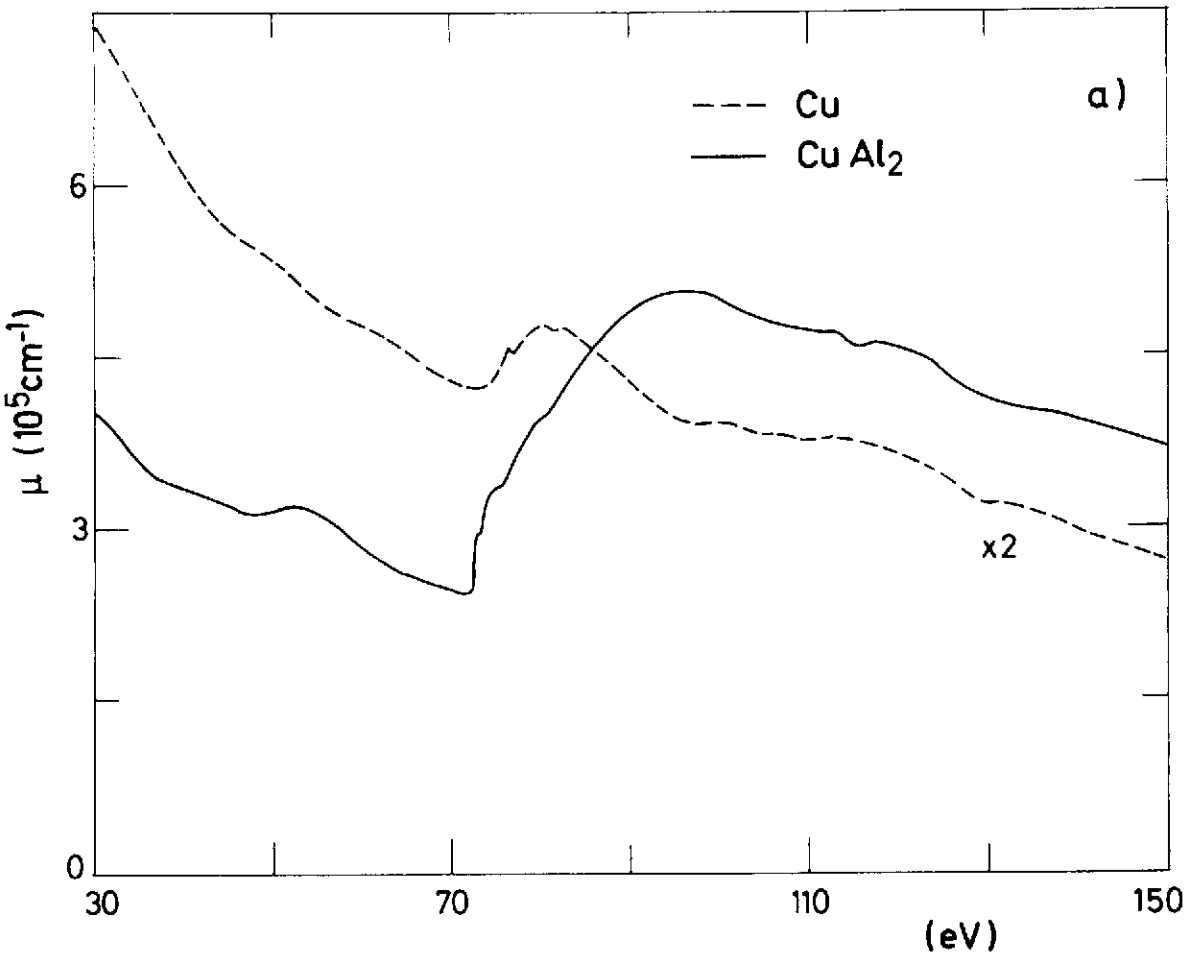
a)
Cu
Cu Al2
x2
μ (10^5cm^-1)
0
3
6
30
70
110
150
(eV)

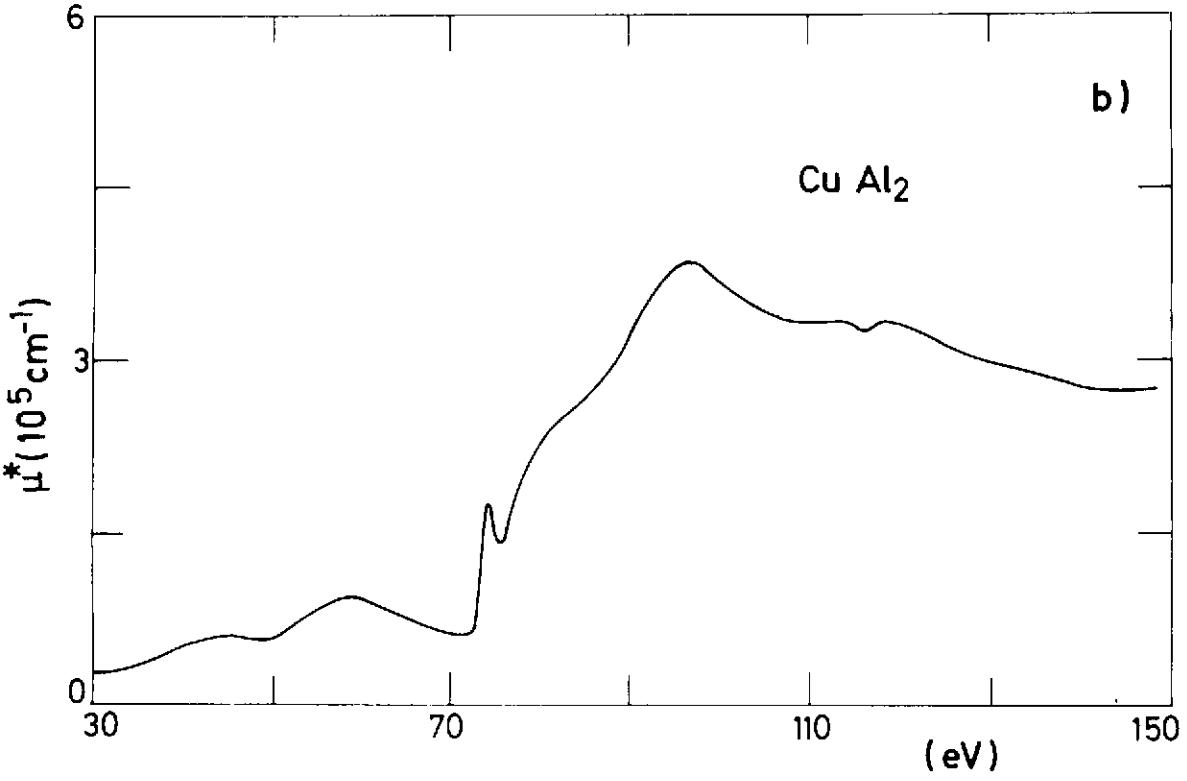
b)
Cu Al2
μ*(10^5cm^-1)
0
3
6
30
70
110
150
(eV)

Fig. 7

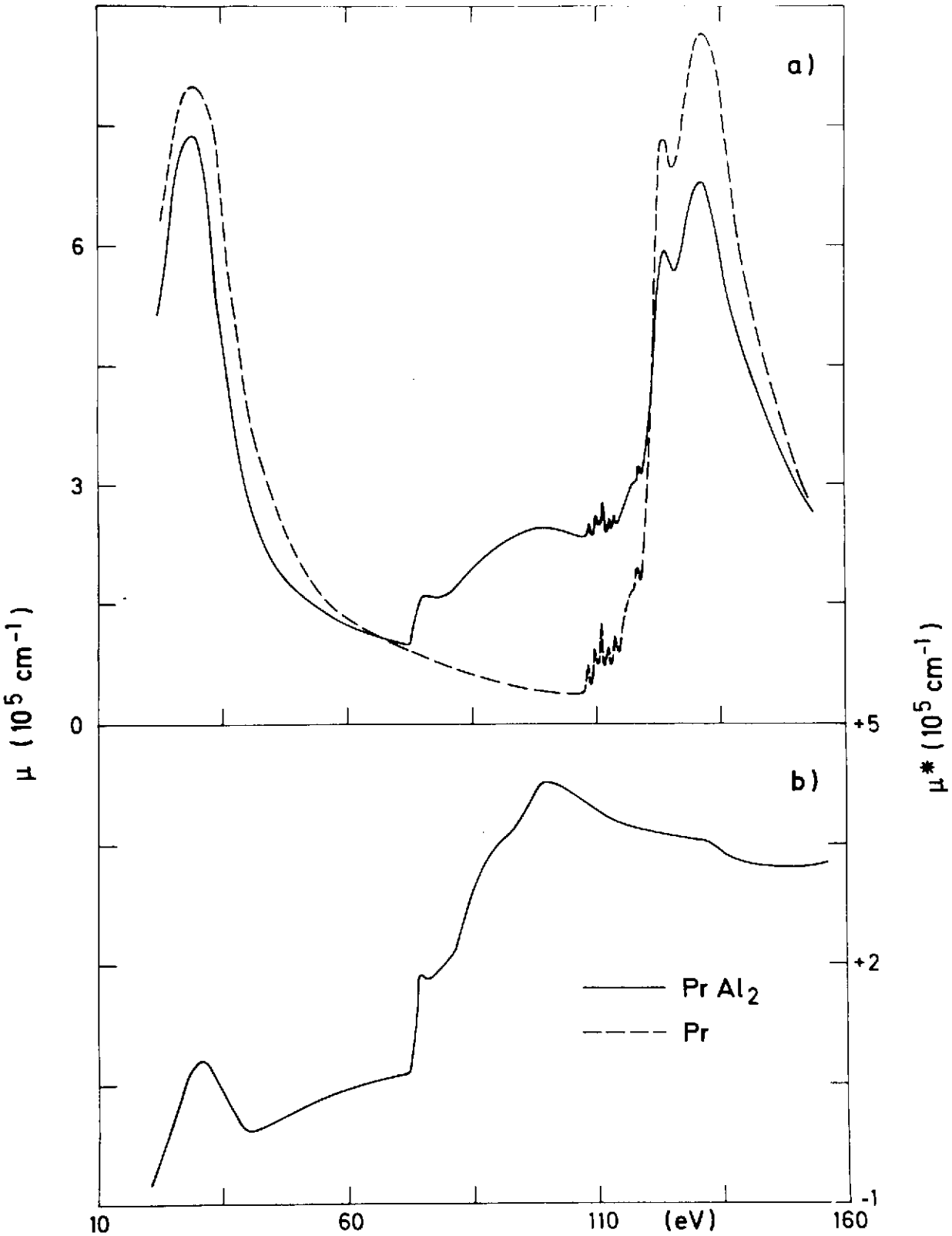

Fig. 8

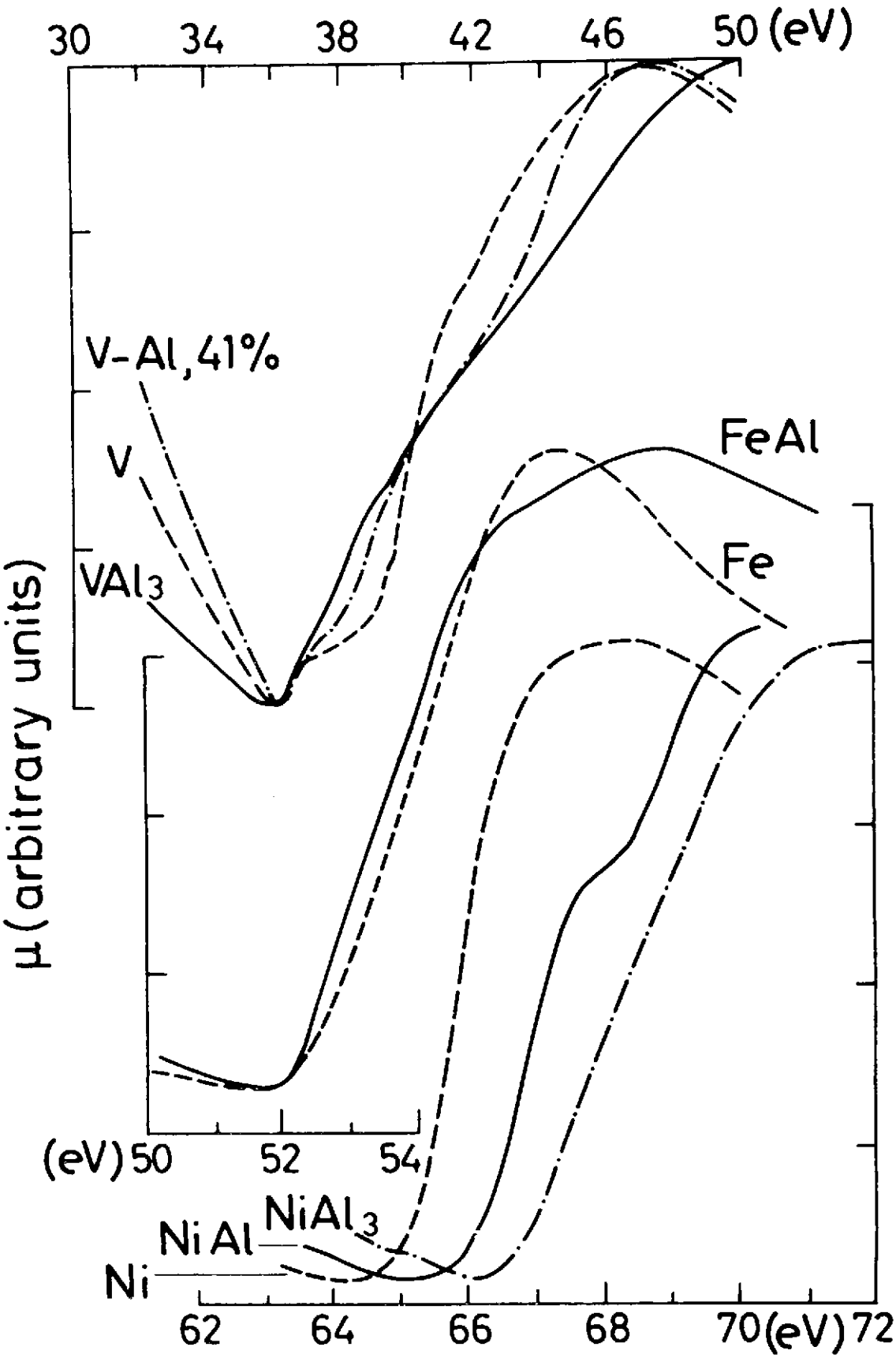
30
34
38
42
46
50 (eV)
V-Al, 41%
V
VAl3
FeAl
Fe
μ (arbitrary units)
(eV) 50
52
54
NiAl3
NiAl
Ni
62
64
66
68
70 (eV) 72

Fig. 9